PETROPHYSICS, VOL. 54, NO. 5 (OCTOBER 2013); PAGE 439–456; 16 FIGURES; 1 TABLE

Major Advancement in Reservoir-Fluid Analysis Achieved Using a New High-Performance Nuclear Magnetic Resonance Laboratory System[1]

R. Freedman[2], V. Anand[2], D. Catina[3], B. Grant[4], P. Tabrizi[2], R. Torres[2], K. Ganesan[2], C. Borman[2], C. Krueckl[2], and D. Ryan[2]

ABSTRACT

A new and innovative high-performance laboratory system for performing low-field nuclear magnetic resonance (NMR) relaxation times and diffusion measurements was built to enable a study of reservoir fluids at the high temperatures and pressures that occur in many oil and gas reservoirs. The primary objective of the study was to determine which reservoir-fluid properties can be predicted from NMR measurements and the accuracy of the predictions. A secondary objective was to determine if combining NMR and near-infrared (NIR) optical absorption data improved the predictions.

Previous industry publications on reservoir fluid studies using NMR are based on measurements acquired using commercial NMR systems. The temperature and pressure specifications and signal-to-noise ratio (SNR) of the new system represent a quantum leap in the technology compared with those of commercially available systems. For the first time, high-quality NMR data on live reservoir fluids can be rapidly acquired at the high temperatures and pressures of worldwide oil reservoirs. The SNR of our system is more than a factor of 15 higher than that of commercial systems so that data acquisition is more than 225 times faster than previously possible. Moreover, the system is easy to maintain and pressure compensation is not required to achieve high pressures. The heart of the system is a compact sensor consisting of an NMR magnet with a low static magnetic-field gradient, a radio-frequency (RF) antenna, and a pair of pulsed-field-gradient (PFG) coils used for NMR diffusion measurements.

The new system was used to acquire a database of hundreds of NMR and optics measurements at different temperatures and pressures on a representative suite of oils typical of those sampled by fluid sampling tools. In addition to the NMR and optics measurements, the database contains measured fluid properties including molecular compositions; saturate, aromatic, resin and asphaltene (SARA) fractions; gas/oil ratio (GOR); viscosity; compressibility; formation volume factor; and density measurements for each oil. The NMR, optics, and fluid-properties measurements were measured at pressures up to 25,000 psi and at temperatures up to 175°C.

The database was used to determine how accurately fluid properties, including molecular composition, SARA fractions, viscosity, GOR, density, and compressibility, can be predicted from NMR measurements. We discuss the laboratory system, sample preparation, measurements, and accuracy of the predictions. We show that each of the aforementioned reservoir fluid properties can be accurately predicted from NMR measurements given the pressure and temperature of the reservoir fluid.

INTRODUCTION

The introduction of pulsed nuclear magnetic resonance (NMR) logging tools in the early 1990s brought to the industry new capabilities for the characterization of oil- and gas-bearing reservoirs. These tools employ diffusion-encoded pulse sequences that can be used to separate oil, gas, and water signals based on contrasts in the molecular diffusion coefficients of the fluids (Akkurt et al., 1996; Coates et al., 1999; Prammer et al., 2001; Looyestijn, 1996; Freedman et al., 2001; Freedman and Heaton, 2004). NMR diffusion-based fluid typing provided the industry with a new tool for identifying oil and gas reservoirs. Additionally, NMR logging provided the density-magnetic resonance (Freedman et al., 1998) method for identifying and evaluating gas-bearing zones. In spite of the successes in fluid typing and the prediction of near-wellbore reservoir fluid volumes, the prediction of accurate reservoir-fluid properties (e.g., composition and fluid density) from NMR has made little progress.

Manuscript received by the Editor August 6, 2013; revised manuscript received October 8, 2013.
[1] Originally presented at the SPWLA 54th Annual Logging Symposium, New Orleans, Louisiana, USA, June 23-26, Paper VV
[2] Schlumberger, 110 Schlumberger Drive, Sugar Land, TX, 77478, USA; Email: freedman1@slb.com, vanand@slb.com, ptabrizi@slb.com, torresr@slb.com, ganesan1@slb.com, cborman@slb.com, ckrueckl@slb.com, dryan3@slb.com
[3] National Oilwell Varco, 10302 Mula Road, Stafford, TX, 77477, USA; Email: dcatina@hotmail.com
[4] Grant Innovation, 618 Mesquite Drive, Cedar Creek, TX, 78612, USA; Email: bill@grantinnovation.com

NMR provides an excellent noninvasive probe for studying the microscopic molecular interactions in fluid systems and, therefore, it provides a means for predicting molecular and macroscopic fluid properties of crude oils. The temperature and pressure dependence of molecular interactions governing the NMR response provides an understanding of the dynamic processes in such systems. Furthermore, measurements of relaxation times and diffusion coefficients of fluids are related to macroscopic properties that are strongly temperature and pressure dependent. Despite the capability of NMR to investigate fluids on the molecular level, little progress has been made in predicting oil properties, such as density, molecular composition, saturate, aromatic, resin, asphaltene (SARA) fractions, and gas/oil ratio (GOR) from NMR.

We believe there are two reasons why such little progress has been made. First, crude oils are complex mixtures of organic and inorganic molecules containing variable and unknown amounts and types of dissolved gas molecules. This complexity cannot be accurately described by the simple, idealized models that are commonly used in the industry (Freedman et al., 2012). It was clear that in order to make real progress in predicting accurate fluid properties from NMR a model-independent approach was needed to deal with the inherent complexity of crude oils. Second, there were no known extensive databases of NMR, pressure-volume-temperature (PVT), and physical properties data acquired on live oils at realistic reservoir conditions. Such databases are critical for the development and validation of the accuracy of NMR-based predictive methods.

The problem of reservoir fluid complexity was addressed by Freedman (2006a) who developed a new model-independent method for accurately solving inverse problems for complex systems. This method uses a general model-independent mapping function to approximate the unknown functional relationship between the NMR measurements and the fluid properties to be predicted. The mapping function can be uniquely determined from a database of NMR and fluid-properties measurements. The mapping function can be expressed in analytical form as a summation of Gaussian radial-basis functions (RBF). The philosophy here is that crude oils are too complex to be accurately described by simple models, however, the physics is contained in the database and it can be represented by a general nonlinear mapping function. Freedman (2006a) tested the mapping function method on a small database of dead oils (oils without dissolved gases) and obtained encouraging results from the predictions of viscosity and molecular composition. It then seemed that it might be possible, using this method, to predict accurate fluid properties of live oils from a database of NMR, PVT, and fluid-properties measurements.

The next step was the installation, in 2005, of a commercial Resonance Instruments Maran NMR 2 MHz spectrometer at the Schlumberger DBR Technology Center in Edmonton, Canada to further assess the viability of the mapping function method when applied to a database of live oils. The NMR spectrometer became part of a laboratory system that included a commercial Temco Inc. pressure cell with some in-house modifications for making NMR measurements on single-phase live oils. The NMR-measurement system, database, and results were discussed recently (Anand and Freedman, 2012). This limited study was encouraging because it proved that important fluid properties, including molecular composition, viscosity, and SARA fractions, could be predicted with reasonable accuracy from a relatively sparse database using the mapping function method. The commercial system had significant limitations and was not a viable system for the acquisition of an extensive database of NMR measurements at realistic conditions of temperature and pressure. The Maran-based system had maximum pressure and temperature limits of 10,000 psi and 110°C, respectively, which fall far short of the pressures and temperatures commonly encountered in oil reservoirs. Another serious limitation of the commercial system was its relatively low signal-to-noise ratio (SNR) (i.e., 15:1), which meant very-long measurement times (e.g., more than 12 hours for pulsed-field-gradient [PFG] diffusion measurements) at each pressure and temperature.

Faced with the limitations of commercial NMR laboratory systems, we designed and built a new high-performance, low-field laboratory NMR system capable of making NMR measurements on live oils at 25,000 psi and 175°C. In this paper, low field refers to a NMR spectrometer with a proton Larmor frequency close to 2 MHz, which is near or above the operating frequencies of the NMR logging tools. It is worth noting that there is negligible frequency dependence for T_1 or T_2 below 2 MHz for crude oils having viscosities in the range typically sampled by fluid sampling tools. At higher frequencies, significant frequency dependence occurs in T_1, which is observed to increase for frequencies above about 10 MHz for crude oils containing asphaltenes (see e.g., Zielinski and Hurlimann, 2011).

It should also be noted that although T_2 has much weaker frequency dependence than T_1, T_2 measurements depend on static gradient, RF field inhomogeneities, etc. and therefore they are typically instrument dependent (Vold et al., 1969). Molecular diffusion (D) is translational motion of the molecule and should be independent of the NMR frequency.

Our high-performance (e.g., SNR of 250:1) laboratory system is, to our knowledge, at the far frontier of low-field NMR technology and is the only system in the world today capable of performing lab NMR measurements on live oils

at 25,000 psi and 175°C. This system was installed at DBR in late 2010 and has been used to acquire a database of hundreds of NMR measurements at different temperatures and pressures on live oils. Additionally, the database contains optical density and fluid properties data acquired on the same suite of oils at the same temperatures and pressures.

The remainder of this paper discusses the key features of the (1) NMR laboratory system, NMR pulse sequences, and the near-infrared (NIR) optics sensor; (2) the database of NMR, NIR optical-density, and fluid-properties measurements on live oils; and (3) the model-independent mapping function method used to predict fluid properties from NMR measurements and discusses the accuracies achieved. The section on the model-independent mapping function method also discusses what, if any, improvement in the accuracies of predicted fluid properties can be achieved by a joint inversion of the NMR and optics measurements.

NMR LABORATORY SYSTEM

Design Limitations of Commercial Low-Field NMR Systems

The current commercial low-field NMR spectrometers for high- pressure and high-temperature applications consist of a pressure cell made of a non-metallic material. The RF coil for transmitting and receiving NMR signals is situated outside the pressure cell. The pressure on the inner walls of the cell is offset by a pressurized, NMR-invisible fluid contained outside the cell. The pressurized fluid reduces the pressure on the inner walls of the pressure cell, and it can also be heated to regulate the temperature of the sample. This design has a number of disadvantages.

First, due to the low filling factor (fraction of the sensor volume that is occupied by the sample), a relatively poor SNR of about 15:1 per acquisition is obtained. The measurements need to be repeated many times and averaged to improve the data quality (Winkler et al., 2004) and therefore the measurements take a very long time.

Second, the commercial systems use thermal exchange with a heated NMR-invisible (hydraulic) fluid to heat the sample under study. This is a very inefficient means of heat transfer and leads to a long thermal-equilibrium time. The time to reach equilibrium increases significantly with the measurement temperature.

Third, the thermal exchange with the hydraulic fluid can lead to differential heating of the sample along its length and, consequently, to convection currents. These currents interfere with the NMR measurements, particularly the diffusion measurements.

Last, the operation and maintenance of the system is very complex. The system requires multiple seals to isolate the pressurized hydraulic fluid and the fluid under study. If the seals fail, the two fluids can mix and destroy the measurement.

Design Features of New NMR System

At the heart of the new system is a novel RF antenna that sits inside a sample holder made of MP35N, a very strong nonmagnetic metallic alloy. The metallic sample holder is capable of handling very high pressures without pressure compensation. This system has been successfully pressure tested to 36,000 psi. The RF antenna consists of a solenoid wound on a slotted titanium antenna frame. The sample holder is sandwiched between a pair of exterior gradient coils used for PFG measurements. The gradient coils produce a linear gradient in the sensitive volume by transmitting low-frequency pulses, which are negligibly attenuated by the metallic sample holder. The assembly sits inside the bore of a permanent magnet custom built to have a small background gradient in the sensitive volume. The fact that the RF antenna is completely submerged in the fluid leads to increased SNR, i.e., more than an order of magnitude higher than that of current commercial low-field NMR systems.

The sensor assembly can be heated in an oven to the required measurement temperature without the need for heat transfer from another fluid. Because the system can be uniformly heated in an oven, no convection currents are induced by temperature gradients. The presence of the metallic sample holder and titanium antenna frame reduces the quality factor (Q) of the RF antenna, thereby leading to a large frequency bandwidth of the antenna. The large bandwidth enables the operation of the system over a wide range of temperatures without the need to retune the antenna to match the Larmor frequency as it decreases with increasing magnet temperature. The NMR sensor is easy to maintain and allows straightforward integration with other sensors, such as optical sensors as subsequently discussed.

NMR Sensor

The sensor of the novel high-pressure, high-temperature NMR instrument consists of the following components.

RF Antenna. The RF antenna for the laboratory system consists of a solenoid coil wound on a nonmagnetic titanium frame. A nonmagnetic antenna frame prevents distortion of the homogeneity of the static magnetic field in the sensitive volume. The RF coil is 1.5 in. long and 0.38 in. in diameter. The antenna sits inside a metallic sample holder. The measurement volume is approximately 8 cm^3. About 80% of the NMR signal comes from the fluid inside of the RF coil (i.e., the sweetspot) and the remainder from the fluid in the annular region between the coil and the sample holder. This design results in an NMR fill factor greater than

1, which greatly enhances the SNR of the measurements. The novel antenna frame has longitudinal slots that allow communication between the fluid inside the RF coil and the fluid outside. This design allows for efficient flushing of the measurement volume, which is critical for obtaining noncontaminated samples during the live-oil charging procedure discussed below.

Sample Holder. The RF antenna resides inside an MP35N metallic tube. This material was chosen for its high strength and resistance to corrosion by reservoir fluids. The magnetic susceptibility of the tube ($\mu = 1.001$) is sufficiently low so that the magnetic-field homogeneity in the sensitive region is negligibly disturbed. The length of the tube is 10.83 in., the inner diameter is 0.65 in. at the center and the outer diameter is 0.875 in. An end-cap made of inconel is threaded to the wide-end of the tube. The sample holder containing the RF antenna is shown in Fig. 1

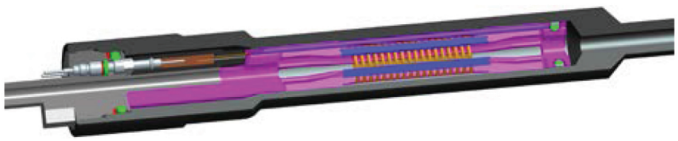

Fig. 1—RF antenna and sample holder. The antenna (magenta) resides inside the metallic sample holder (gray). The electrical connection with the antenna is provided by two connectors (i.e., pressure-feed through pins shown in light gray).

Pulsed-Field-Gradient Coils. A pair of gradient coils is used to create a magnetic-field gradient in the sensitive region for pulsed-field-gradient (PFG) diffusion measurements. The coils consist of an elliptically shaped Maxwell pair embedded in two PEEK fixtures. The coils carry current in opposite directions and create a linear magnetic-field gradient in the measurement volume. The length of the coils is 2.6 in. and the width is 0.8 in. The sample holder is sandwiched between the PEEK fixtures containing the coils as shown in Fig. 2.

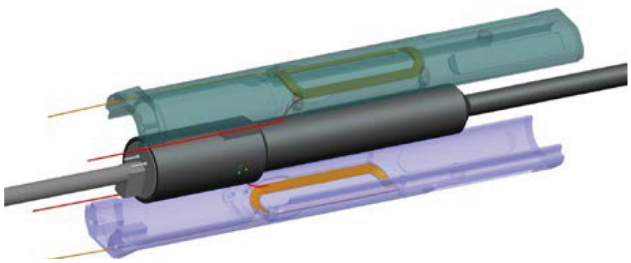

Fig. 2—Gradient coils encapsulate the metallic sample holder.

The sample holder and gradient coils fit inside the bore of a permanent magnet used for NMR measurements. The low-frequency PFG pulses are negligibly attenuated by the metal sample holder. However, the pulses generate eddy currents in the sample holder, which can affect the phase of the NMR echoes. The effect of eddy currents was experimentally investigated and found to be negligible if the duration between gradient pulses and echoes is greater than 1.5 msec.

A linear relationship between the current in the gradient coils and the corresponding magnetic-field gradient in the measurement volume was experimentally determined prior to performing diffusion measurements. The linear relationship serves as a calibration for the PFG diffusion measurements. The linear relationship was obtained at room temperature using bipolar diffusion-editing pulse sequences with a fluid (water) of known diffusivity. The bipolar PFG pulse sequence exactly cancels the cross term containing the scalar product of the static magnetic field gradient of the NMR magnet and the applied pulsed field gradient (Freedman and Ganesan, 2007). The cross term, which is present in the conventional Stejskal-Tanner PFG sequence (Stejskal and Tanner, 1965), causes systematic errors in the measured diffusion coefficients if bipolar sequences are not used.

The calibration was validated by using it to measure the diffusivity of water at multiple temperatures up to 175°C. The results agree with the literature results of Krynicki et al. (1978) to within 4% accuracy, confirming that the calibration has no temperature dependence and remains valid to 175°C. The accuracy of PFG measurements was further validated by performing diffusion measurements with hexane at multiple temperatures and pressures for which the literature value of the diffusivity is known (Harris, 1982). We achieved agreement with literature values to better than 4%.

NMR Magnet. A compact samarium cobalt (SmCo) permanent magnet with a field-strength of 535 G at room temperature and a low static magnetic-field gradient in the measurement volume was custom designed and built for NMR measurements. The field strength corresponds to a proton Larmor frequency of 2.28 MHz. The magnet assembly is an 8 in. cylinder with a 3.6 in. outer diameter. The magnet consists of a central bore with a 1.4 in. diameter that houses the sample holder, including the RF antenna and the gradient coils. The magnetic assembly is shown in Fig. 3.

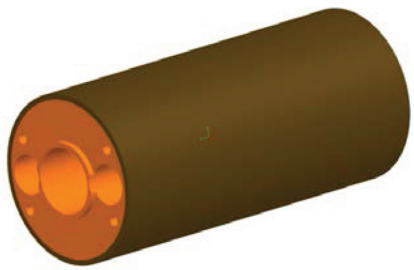

Fig. 3—A picture of the NMR magnet assembly.

The magnet assembly contains two spatially separated parallel plates made from nonmagnetic stainless steel. On each plate there are situated SmCo magnets each magnetized perpendicular to the plate. The magnetic-field variations in the measurement region between the plates are smoothed by magnetic-pole pieces situated below and adjacent to each plate. This design creates a magnetic field in a direction transverse to the axial direction of the sample holder. The static magnetic-field gradient in the measurement volume is relatively small, which enables accurate and precise measurements of the long T_2 values observed in reservoir fluids. The magnet assembly is contained in a cylindrical magnetic shell that provides a return for the magnetic flux.

The static magnetic field gradient over the sample volume was measured at multiple temperatures from room temperature to 175°C. The average magnetic field gradient in the NMR sensitive region was less than 1 G/cm for all temperatures.

NMR Pulse Sequences. The NMR system has a fully programmable pulse sequencer and is capable of performing all the standard low-field NMR relaxation times and diffusion measurements. The live-oil database consisted of T_1, T_2, and diffusion measurements on each sample at each temperature and pressure. The measurements performed were:

(1) Carr-Purcell-Meiboom-Gill (CPMG) measurements of T_2,
(2) saturation recovery/CPMG for simultaneous measurement of T_1 and T_2,
(3) bipolar PFG/CPMG for simultaneous measurement of diffusion (D) and T_2.

The CPMG acquisitions were phase-alternated pairs (PAP) used to eliminate DC offsets as well as any ringing caused by the 180° pulses. The wait-time preceding each CPMG measurement was at least 5 times the maximum longitudinal-relaxation time in the sample.

The saturation recovery/CPMG sequences consisted of a suite of PAP echo trains that were acquired using different recovery times. Prior to each recovery time the longitudinal magnetization was driven toward zero by application of a series of 90° RF pulses plus a few spoiler gradient pulses. Following each recovery time a CPMG echo train was acquired. A suite of measurements typically included about 12 recovery times selected to be equally spaced on a logarithmic scale. This suite of measurements was simultaneously inverted to produce a two-dimensional (2D) T_1-T_2 map.

The Stejskal-Tanner PFG technique is the preferred method for accurately measuring molecular diffusion coefficients for liquids. The bipolar PFG pulse sequence used in our laboratory system provides accurate measurements of D and diffusion-free measurements of T_2 in the presence of the static gradient of the NMR magnet. The bipolar PFG sequence is shown in Fig. 4.

Note that four gradient pulses are applied before the diffusion-encoded spin-echo is observed. The diffusion-encoded spin-echo is refocused by applying a train of 180° pulses to produce a sequence of spin-echoes whose amplitudes decay with relaxation time T_2. It can be shown that the measurement kernel describing the bipolar PFG is the same as the kernel for a unipolar PFG except for an extra factor of 2, which results from the application of four gradient pulses instead of two (the detailed derivation is given by Freedman and Ganesan, 2007).

A 2D diffusion and relaxation-time measurement consisted of a suite of PFG sequences. The different PFG sequences in a suite were acquired using different gradient pulse widths (δ), gradient amplitudes (g), and diffusion times (Δ) to vary the diffusion attenuation. This suite of PFG measurements was simultaneously inverted to produce a 2D D-T_2 map (Freedman, 2006b).

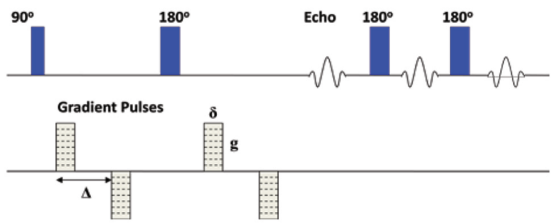

Fig. 4—Bipolar pulse-field-gradient sequence used to measure molecular diffusion distributions.

Optics Sensor. An optical cell rated to 175°C and 25,000 psi was installed in the sample flow path in order to measure the NIR transmission absorption spectra of live crude oils at reservoir conditions. The cell was secured against the body of the oven to prevent artifacts in the data caused by oscillations or vibrations. The absorption spectra of live oils were measured in the wavelength range from 400 to 2200 nm in 1-nm increments. The spectrum was measured at each temperature and pressure for which the NMR measurements were made. The baseline spectrum of the optical cell, measured with pressurized N_2 at 500 psi and the corresponding temperature, is subtracted from the absorption spectrum of the live oil to remove the absorption contribution from the cell. The optical density is defined as the logarithmic ratio of the incident- (I_o) and transmitted- (I_t) light intensities.

NMR, NIR OPTICAL-DENSITY, AND FLUID-PROPERTIES MEASUREMENTS

An extensive database of NMR, optical density, and

fluid-properties measurements was acquired on a suite of 18 live oils at multiple temperatures and pressures. To include oils with a wide range of fluid properties such as viscosity, GOR, and SARA fractions in the database, the oil samples were obtained from petroleum reservoirs in geographical locations around the world including the South America, North Sea, Canada, USA, Gulf of Mexico, Middle East, Alaska, Malaysia, and Africa. Measurements were made over a wide temperature and pressure range to analyze the properties at representative reservoir conditions. The following sections describe the procedure for charging live-oil samples in the system as well as the database of fluid properties, NMR, and NIR optical-density measurements.

Sample Charging

The live-oil samples were prepared by equilibrating the samples for one to five days in a pressure cell at a known GOR. The NMR and optical sensors were installed inside an oven while the electronics were kept outside. Metal flowlines connect the NMR sample holder and the optical cell to inlet and outlet valves mounted on the outside of the oven. The fluids are injected into the system through the inlet valve using a hydraulic pump. The outlet port is used to collect the effluents.

The protocol for charging the live-oil sample includes the following steps. The NMR and optical sensors are heated inside the oven to the specified measurement temperature until thermal equilibrium is established. The flowlines are evacuated and purged with pressurized N_2 to remove any traces of fluid. Subsequently, a buffer fluid at 10,000 psi is injected into the flowlines through the inlet port. The buffer fluid is the dead stock-tank oil (STO) used to synthesize the live oil. The purpose of the buffer fluid is to maintain the pressure in the flowlines and the NMR sample holder above the bubblepoint pressure of the live oil. At least two fluid-system volumes of live fluid are injected quasi-statically into the system.

The described sample charging protocol was validated prior to acquisition of the database as follows. A typical database oil was selected and time-lapsed NMR D-T_2 measurements were performed as the STO was gradually flushed by the live oil. These measurements were performed to verify that the live oil would remain as a single-phase fluid during the charging procedure. The absence of a separate peak for free gas in the D-T_2 map confirmed that the live oil remained in a single phase during charging. The composition of the effluent at the outlet port was also measured after injecting fixed volumes of the live oil. It was further validated that the composition of the effluent exactly matched the composition of the live oil after injecting two system volumes.

Fluid-Properties Measurements

A wide variety of fluid-properties measurements were made on the live oils in the database. Fluid properties that depend on temperature and pressure (e.g., density, viscosity, compressibility) were measured at three temperatures of 75-, 125-, and 175-°C and at multiple pressures. Brief descriptions of the fluid-properties measurements are included below.

Viscosity. The viscosity of live oils was measured at the three temperatures by using an electromagnetic viscometer. At each temperature, viscosity measurements were made at multiple pressures above the saturation pressure and up to a maximum pressure of 20,000 psi. The upper limit was constrained by the pressure rating of the viscometer. The range of live oil viscosities included in the database covered almost three orders of magnitude, from 0.1 to 80 cp.

Fluid Density. The mass density of the live oils was measured at the three temperatures and at multiple pressures using a commercial density cell rated to a maximum pressure of 20,000 psi. The live-oil densities ranged from 0.44 to 0.93 g/cm^3.

Molecular Composition. The molecular composition was measured using gas chromatography (GC). The molar and weight fractions of components with carbon number ranging from C_1 to C_{29} and a C_{30+} residual fraction were measured.

Gas-Oil Ratio. The GOR was measured at standard conditions using a laboratory gasometer. The GORs of the live oils in the database ranged from 150 to 3,000 scf/bbl.

Bubblepoint. The bubblepoint pressures of the single-phase live oils were measured at the three temperatures using a constant composition expansion (CCE) instrument.

Fluid Compressibility. The isothermal fluid compressibility (β) measures the relative volume change of the live oil as a response to pressure change. Fluid compressibility was measured using the CCE instrument at the three temperatures and multiple pressures up to a maximum pressure of 20,000 psi.

Asphaltene Onset Pressure (AOP). AOP is defined as the pressure at which the asphaltenes precipitate from the live oil at a given test temperature as the pressure is decreased. AOP was measured at the three temperatures using a solids detection system.

SARA. SARA is the fraction of saturates, aromatics, resins, and asphaltenes measured in a dead-oil sample. SARA was measured on all 18 oils in the database.

NMR Measurements

NMR measurements were performed on live-oil samples at three temperatures of 75-, 125-, and 175-°C. At each temperature, measurements were performed at multiple

pressures above the bubblepoint and asphaltene onset pressures of the live oil at that temperature. At 125 and 175°C, measurements were performed up to a maximum pressure of 25,000 psi. However, at 75°C, the maximum measurement pressure was 15,000 psi, in most cases, or 20,000 psi in some cases. The lower pressure limit at 75°C was used because reservoirs at low temperatures are also typically at lower pressures. Three types of NMR measurements were made at each temperature and pressure: CPMG, T_1-T_2 and D-T_2. The echo data were inverted to obtain T_2 distributions and 2D T_1-T_2 and D-T_2 maps. One-dimensional T_1 and D distributions were also obtained from the projections of the 2D maps along the T_1 and D dimensions. In total, the database consisted of 462 NMR CPMG, T_1-T_2 and D-T_2 measurements made on 18 live oils at multiple temperatures and pressures. It is worth noting that the 18 oils selected for the database have viscosities and GORs in the same range, as do the oils typically sampled by borehole fluid sampling tools. Results for a few typical oils in the database are described next.

Example Oil 1. This oil sample was obtained from a reservoir in the North Sea and has a relatively low GOR of 207 scf/bbl. The D-T_2 maps measured at the three temperatures and multiple pressures are shown in the left panel of Fig. 5. The peaks in the D-T_2 maps lie along the dead-oil line (Freedman et al. 2001),

$$D = \lambda T_2, \tag{1}$$

where $\lambda = 5 \cdot 10^{-6}$ cm^2/s^2. The values of D and T_2 increase with temperature because of the increased mobility of the molecules with temperature. In contrast, D and T_2 decrease with pressure because of reduced mobility of fluid molecules under pressure. The pressure dependence of T_2 is also consistent with the increase in viscosity and rotational correlation time with the increase in pressure.

The T_1-T_2 maps for the oil at the corresponding temperatures and pressures are shown in the right panel of Fig. 5. The logarithmic mean $\langle T_1 \rangle$ and $\langle T_2 \rangle$ were computed from the 1D T_1 distribution and the diffusion-corrected T_2 distribution obtained from the D-T_2 maps. The $\langle T_1 \rangle / \langle T_2 \rangle$ ratio is greater than unity—albeit not significantly—at all temperatures and pressures with an average value of 1.3. It has been shown empirically (Zhang et al., 2002) that the deviation of the $\langle T_1 \rangle / \langle T_2 \rangle$ ratio from unity in crude oils is caused by enhanced T_2 relaxation by paramagnetic atoms on the asphaltene molecules. The enhanced average value of 1.3 for the $\langle T_1 \rangle / \langle T_2 \rangle$ ratio for Oil 1 indicates the presence of asphaltenes. The laboratory analysis shows that this oil contains 1.5 wt% asphaltenes.

Example Oil 2. Oil 2 was obtained from a reservoir in Africa and has a significantly higher GOR (1500 scf/bbl)

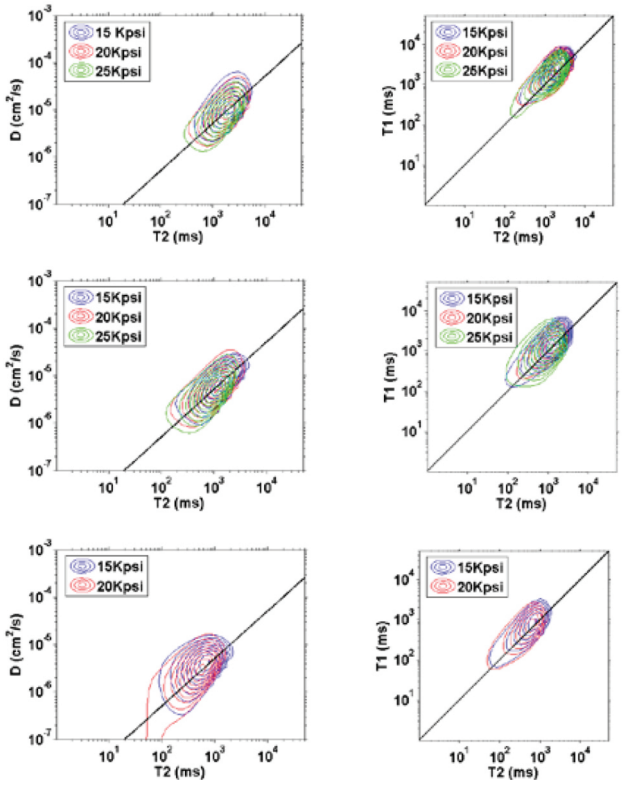

Fig. 5—D-T_2 maps (left panel) and T_1-T_2 maps (right panel) for Oil 1 in the database. The maps are shown for three temperatures: 175°C (top), 125°C (middle), and 75°C (bottom). The peaks in the D-T_2 maps lie on the dead-oil line.

compared with Oil 1. Figure 6 shows the D-T_2 and T_1-T_2 maps at multiple temperatures and pressures. The peaks in the D-T_2 maps for this sample lie to the left of the dead oil line, Eq. 1. This deviation arises because the dead-oil line is based on the empirical correlation between diffusion and T_2 for dead oils. The gas in this high-GOR oil causes faster T_2 relaxation that reduces T_2 and shifts the signal to the left of the dead-oil line (Lo et al. 2000; Freedman and Heaton 2004).

The average $\langle T_1 \rangle / \langle T_2 \rangle$ ratio for Oil 2 is 1.2 which is smaller than that for Oil 1. This observation suggests that Oil 2 contains smaller amounts of asphaltenes than Oil 1 (Hurlimann et al., 2009). This conclusion is also consistent with the fact that the presence of substantial quantities of nonpolar gaseous components such as methane reduces the solubility of polar asphaltene molecules. The laboratory analysis shows that Oil 2 contains only 0.1 wt% asphaltene compared with 1.5 wt% in Oil 1.

Example Oil 3. Oil 3 was obtained from a reservoir in Colombia. This oil has a moderate GOR (1053 scf/bbl) and contains 0.8 wt% asphaltene content. Figure 7 shows the D-T_2 and T_1-T_2 maps for Oil 3 at multiple temperatures and pressures. In this oil "the slope of the peaks" (e.g., the slope

of a line drawn from the T_2 axis through the center of the cloud of signal amplitudes in a 2-D map) in the D-T_2 map deviate significantly from the dead-oil line. This deviation is the result of reduced T_2, which for this oil can be caused by two separate and independent effects. The first effect is faster T_2 relaxation caused by dissolved gas as discussed previously. Another effect for Oil 3 could be enhanced T_2 relaxation caused by the presence of paramagnetic ions, such as vanadium, that are situated in the asphaltene molecules. The enhanced relaxation caused by asphaltenes was discussed by Hurlimann et al. (2009) who measured D-T_2 maps on a suite of dead oils. These authors postulated that the asphaltene molecules interact with other nearby oil molecules (i.e., maltenes) and slow down their rotational motion, which leads to faster T_2 relaxation. These authors also observed that T_1 relaxation is much less affected by interactions with the asphaltenes so that the observed $<T_1>/<T_2>$ ratios are also greater than one. Hurlimann et al. (2009) also reported that diffusion of the maltenes was observed to not be affected by the presence of the asphaltenes up to 4.7 wt%.

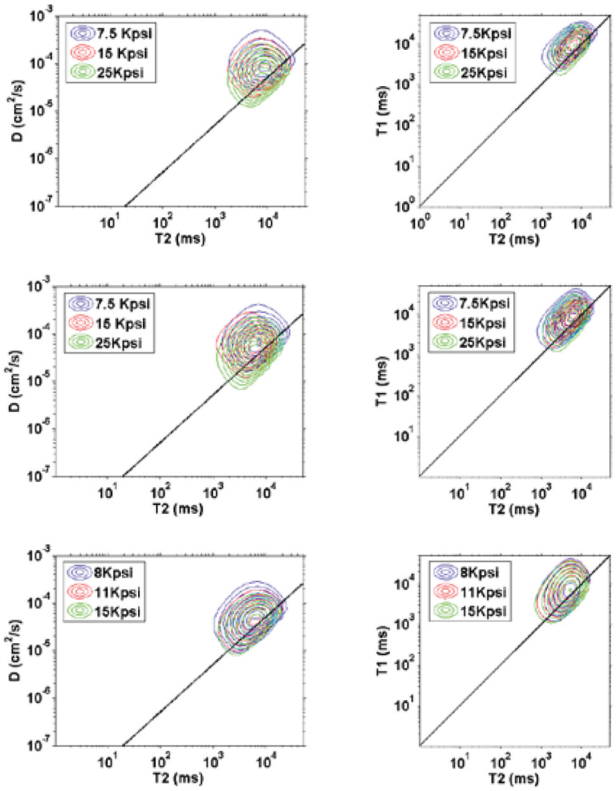

Fig. 6—D-T_2 maps (left panel) and T_1-T_2 maps (right panel) for Oil 2 in the database. The maps are shown for three temperatures: 175°C (top), 125°C (middle), and 75°C (bottom). The peaks in the D-T_2 maps lie to the left of the dead-oil line because of the enhanced diffusion and relaxation of gaseous components.

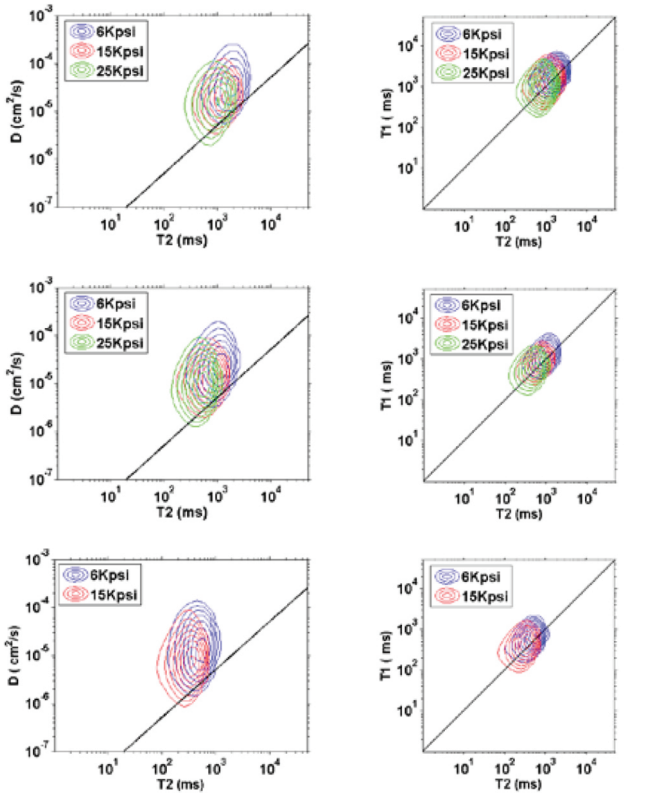

Fig. 7—D-T_2 maps (left panel) and T_1-T_2 maps (right panel) for Oil 3 in the database. The maps are shown for three temperatures: 175°C (top), 125°C (middle), and 75°C (bottom). The slope of the peaks in the D-T_2 maps deviate significantly from the dead-oil line.

Our results on live oils show that the slope of the peaks is independent of pressure at each temperature. However, the slope gradually decreases with increase in temperature. This observation suggests that the relaxation strength of the asphaltene molecules decreases with the increase in temperature. It is worth noting that the slope cannot be correlated with asphaltene concentration. This conclusion follows from the fact that Oil 1 has higher asphaltene content than does Oil 3, yet the D-T_2 maps for Oil 1 exhibit a much smaller slope. The relaxation strength of the asphaltene molecules clearly depends not only on their concentration in the oil but also on where the paramagnetic ions are situated within the asphaltene molecule.

The analysis of T_1-T_2 maps for Oil 3 shows that the $<T_1>/<T_2>$ ratios are larger than those for Oils 1 and 2. Furthermore, in contrast to Oils 1 and 2, the $<T_1>/<T_2>$ ratio for Oil 3 decreases with temperature. The average values are 1.43 at 75°C, 1.37 at 125°C, and 1.32 at 175°C. The decrease in T_1/T_2 ratio is consistent with the previous conclusion that the relaxation strength of asphaltene molecules decreases with increase in temperature.

The NMR responses of the three example oils shows that the temperature and pressure dependence of D and relaxation time distributions in crude oils is complex and depends on

the detailed molecular composition of the oil. We did not attempt to apply a physical model to the interpretation of the diffusion and relaxation-time measurements because it would be difficult to accurately understand the complex physics with simple models.

NIR Optical-Density Measurements. Figure 8 shows the absorption spectrum for Oils 1 and 2 at 175°C and multiple pressures. The spectrum is shown in the NIR wavelength range from 1,500 to 2,000 nm. The molecular absorption peaks at 1,700 nm correspond to the resonance of the C-H bond. The figures show that the effect of increasing pressure is to increase the amplitude of the optical density without changing the shape of the absorption spectrum. The optical density increases with pressure because of the increase in the density of the oil.

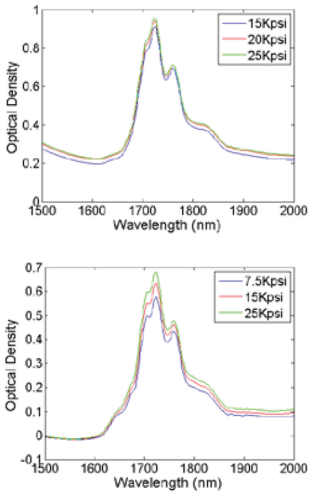

Fig. 8—Absorption spectra for (top) Oil 1, and (bottom) Oil 2, at 175°C and multiple pressures.

METHOD FOR PREDICTING ACCURATE RESERVOIR FLUID PROPERTIES

Crude oils are complex mixtures consisting of dissolved gases and various other hydrocarbon and inorganic molecules of unknown sizes, shapes, and types. The physics of such complex mixtures cannot be accurately described by simple idealized models, e.g., linear-chain models that ignore the presence of aromatic, asphaltene, and other nonlinear hydrocarbon molecules.

For this study we developed and used a novel model-independent method to predict accurate fluid properties of live-oil samples given NMR measurements, pressure, and temperature. To our knowledge there are no alternative methods that can provide accurate fluid properties predictions, or for that matter, even make any predictions for most of the fluid properties of interest.

The model-independent method uses the database of NMR and laboratory fluid-properties measurements that we acquired on a representative suite of live-oil samples. The database is divided into input measurements such as NMR measurements, pressure, and temperature and output measurements such as viscosity, density, molecular composition, and SARA for each oil sample. The unknown functional relationship between the input measurements and the outputs is approximated by a general nonlinear mapping function that can be uniquely determined from the database. The method is flexible and allows combining measurements from multiple sensors, for example, NMR and optics. The philosophy underlying the method is that the physics is contained in the database and the unknown functional relationship can be approximated by the RBF mapping function, which can accurately represent any smooth and continuous nonlinear function. The mapping function is an analytical function that can be constructed from the database without iterative training. It can be written as a linear combination of RBFs as discussed by Freedman et al. (2012).

The RBF mapping functions used to predict live-oil properties in this study can be written in the general form

$$\vec{F}(\vec{x}) = \frac{\sum_{i=1}^{N} \vec{c}_i \exp\left(-\frac{\left\|\vec{x}-\vec{x}_i\right\|^2}{2s_i^2}\right)}{\sum_{i=1}^{N} \exp\left(-\frac{\left\|\vec{x}-\vec{x}_i\right\|^2}{2s_i^2}\right)}. \quad (2)$$

The mapping function $\vec{F}(\vec{x})$ represents the fluid property to be predicted, e.g., molecular composition, viscosity, etc. Note that for multicomponent oil properties, such as molecular composition, the mapping function is a vector whose elements are the mole fractions of the different carbon numbers whereas for single-component oil properties such as viscosity, it is a scalar function.

The summations in the equation are over the number of measurements N in the database. The database inputs for the i-th measurement are contained in the vector $\vec{x}_i$ and the vector $\vec{x}_i$ contains the input measurements made on an unknown sample whose fluid properties are to be predicted. The expansion coefficients $\vec{c}_i$ can be uniquely determined from the database. The arguments of the Gaussian functions are the Euclidean distances in the input measurement space between the unknown input measurement vector $\vec{x}$ and the database input measurement vector $\vec{x}$:

$$\| \vec{x} - \vec{x}_i \|^2 = \sum_{k=1}^{N_c} (x_k - x_{k,i})^2, \quad (3)$$

where N_c is the number of components in the vector of input measurements. Optimal widths s_i for the Gaussian functions

can be determined from the nearest neighbor distances.

Fluid Properties Predictions and Accuracies From NMR Measurements

Viscosity. The dependence of NMR relaxation in fluids on the fluid viscosity is very well known for pure fluids. In that case, the relaxation rate is proportional to the ratio of the fluid viscosity (η) and the temperature:

$$\frac{1}{T_1} = \frac{1}{T_2} \propto \frac{\eta}{T}. \quad (4)$$

This relationship is valid within the extreme narrowing regime for which the product of Larmor frequency and molecular rotational correlation time is significantly less than 1. Similarly, the diffusivity of spherical particles in a dilute solution is also related to the viscosity as elucidated by the Stokes Einstein equation

$$D = \frac{k_B T}{6\pi\eta a_s}. \quad (5)$$

Here a_s is the radius of the diffusing spherical particles, k_B is Boltzmann's constant, T is the temperature in degrees Kelvin, and η is the viscosity of the solvent. The dependence of live-crude-oil viscosities on relaxation time and diffusivity distributions is, however, complex and depends on the detailed molecular composition of the crude oil, temperature, and pressure. The existing empirical correlations that are used to predict live-crude-oil viscosities from NMR measurements are based on simple alkane mixture models (Lo et al., 2000). Such simple empirical models do not accurately describe crude oils, which are extremely complex mixtures with varying compositions.

The model-independent mapping function technique allows accurate prediction of live-crude-oil viscosities from NMR measurements and therefore overcomes the limitations of simple empirical models. It follows from Eq. 2 that a mapping function for predicting live crude oil viscosities from NMR T_1, T_2, and D distributions, temperature, and pressure can be written in the form

$$\eta = \frac{\sum_{i=1}^{N} c_i \exp\left(-\frac{||\vec{A}_T - \vec{A}_{T,i}||^2}{2s_i^2}\right)}{\sum_{i=1}^{N} \exp\left(-\frac{||\vec{A}_T - \vec{A}_{T,i}||^2}{2s_i^2}\right)}. \quad (6)$$

Here is a vector $\vec{A}_T$ that includes the amplitudes of the T_1 distribution $A(T_1)$, T_2 distribution $A(T_2)$, diffusivity distribution $A(D)$, temperature, and pressure of a live-crude-oil sample whose viscosity is to be predicted

$$\vec{A}_T = \vec{A}_T(A(T_1), A(T_2), A(D), T, P). \quad (7)$$

In Eq. 6 $\vec{A}_T$ is a vector that contains the inputs for the i-th sample in the database. Note that a sample is defined by the database measurements made on a specific crude oil at a particular temperature and pressure. The amplitudes of the T_1, T_2, and D distributions are normalized with the respective largest values in the distribution to eliminate the dependence of the amplitudes on the hardware and software settings. Temperature and pressure are also normalized with the largest respective values in the database. The dimensionality of the input vector is the sum of the number of components in the T_1, T_2, and D distribution plus 2. The widths of the Gaussian functions (s_i) are computed to be proportional to the nearest neighbor distances in the database input:

$$s_i = \alpha(NN)_i. \quad (8)$$

where $(NN)_i$ is the nearest neighbor Euclidean distance for the i-th sample in the database. In practice the proportionality factor α is determined from the database as discussed below.

The accuracy of the predictions was validated by applying the methodology to the database itself. The validation was done by using the "leave-one-out" method. In this method, the measurements at all temperatures and pressures made on each live oil are sequentially removed from the database, and a mapping function, Eq. 6, is constructed between viscosity and input measurements for the remaining database samples. The predicted viscosities of the live-crude oil that was removed from the database are obtained from the mapping function using the input measurements made on this crude oil at multiple temperatures and pressures. Note that the NMR measurements made at pressures higher than 20,000 psi were not included in the database for the construction of the mapping function because the laboratory viscosity values were measured up to a maximum pressure of 20,000 psi. Furthermore, the measurements made on Oil 3 were also not included because the relaxation time distributions of this oil are affected by the presence of paramagnetic ions. Because the database did not contain other crude oils with such large concentration of paramagnetic ions, the NMR relaxation times for this oil are not well represented by the remaining crude oils in the database.

The predictions were obtained by using different combinations of T_1, T_2, and D distributions included in the input vector. The accuracies of the results were comparable in all cases. However, the best predictions were obtained for the case in which the input vector consisted of the normalized T_1 and D distribution and normalized T and P. Figure 9 shows the comparison of predicted live-crude-oil viscosities with the viscosities measured in the laboratory. The comparison for predicted and measured viscosities is shown for 113 measurements made on 17 live oils in the

database. The optimal α was determined by simple trial and error by minimizing the deviation between predicted and measured viscosities. The optimal value of α was 0.9. Viscosity predictions were obtained within an average accuracy of 10.6% over the entire viscosity range. This accuracy is exceptionally good considering that there were no adjustable parameters in the estimation and the range of viscosity values covered almost three orders of magnitude.

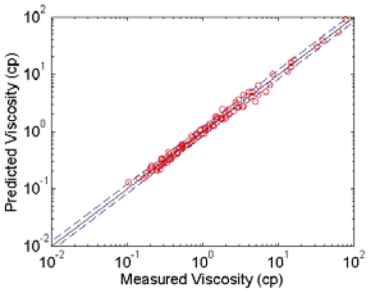

Fig. 9—Comparison of live crude oil viscosities predicted from T_1 and D distributions, T, and P using the RBF mapping function method with the values measured with a viscometer in the laboratory. The solid black line is the equal-value line and the blue dashed lines are located at 20% deviation. The viscosities are predicted to within 10.6% average accuracy over the entire range.

Because the diffusion distribution is not affected by the presence of paramagnetic ions, the viscosities of live oils were also predicted using the D distributions, T, and P in the input vector and including Oil 3 in the database. In this case, viscosities were predicted within an average accuracy of 12.7%.

Density. The dependence of relaxation time and diffusivity of *n*-alkanes on the density has been studied extensively in the literature (Von Meerwall et al., 1998). The relaxation time and diffusivity of pure fluids decrease with density in a nonlinear fashion. The prediction of live-crude-oil density from NMR relaxation time and diffusion distributions has never been studied, and no analytical or empirical models exist for prediction of density from NMR measurements.

The mapping function methodology can be easily applied for quantitative prediction of live-crude-oil density from NMR measurements. Similar to Eq. 6, the density of live-crude oils is expressed as a linear combination of normalized Gaussian RBFs. The input vector $\vec{A}_T$ of the Gaussian functions consists of normalized T_1, T_2, and D distributions, and normalized T and P. Figure 10 shows the comparison of the live oil densities predicted using the leave-one-out method with the values measured in the laboratory. Oil 3 was excluded from the database for the construction of the mapping function. The optimal α determined from trial and error was 1.0. The density is predicted to within an average absolute accuracy of 0.019 g/cm^3. The results show for the first time that density of live-crude oils at reservoir conditions can also be accurately predicted from NMR measurements.

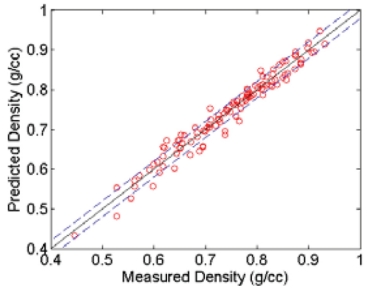

Fig. 10—Comparison of live crude oil densities predicted from T_1, T_2, and D distributions, T, and P using the RBF mapping function method with the values measured in the laboratory. The solid black line is the equal-value line and the blue dashed lines are located at 0.02 g/cm^3 deviation. The densities are predicted to within 0.019 g/cm^3 average absolute accuracy over the entire range.

Compressibility. The isothermal coefficient of compressibility is an important fluid property required for the solution of transient fluid-flow problems, design of high-pressure surface equipment, prediction of acoustic wave velocities in crude oils, and material-balance calculations. The direct measurement of compressibility in the laboratory using PVT analysis is expensive and time consuming. Empirical models have been developed to predict compressibility of live-crude oils from other fluid properties such as bubblepoint and density. However, these models suffer from several fundamental limitations. They are too simple to be accurate, lack generality, and contain empirical parameters that can vary over a wide range.

A mapping function was constructed to predict compressibility of live-crude oils from measured NMR distributions. The input vector for the mapping function consisted of normalized T_1, T_2, and D distributions, and normalized T and P. Figure 11 shows the comparison of the live-crude-oil compressibilities predicted using the leave-one-out method with the values measured in the laboratory. The compressibility values are predicted within an average accuracy of 8.4%. The optimal α is 2.0. In this case, the addition of measurements made on Oil 3 in the database was not found to deteriorate the accuracy of predictions.

Formation Volume Factor (B_o). The formation volume factor of live-crude oils is a measure of the shrinkage or reduction in the volume of the oil as it is produced. Accurate prediction of formation volume factor is crucial for the calculation of oil reserves and oil in place under stock tank conditions. The expression for the calculation of formation volume factor is,

$$B_o = \frac{\text{Vol. of oil+gas @ reservoir press. and temp.}}{\text{Volume of stock tank oil}} \quad (9)$$

Empirical equations have been proposed to predict formation volume factor from compressibility and bubblepoint. These equations are approximate and require the knowledge of other fluid properties such as compressibility and bubblepoint.

The values of the formation volume factor can be exactly calculated from density and GOR of the live-crude oils by using material balance:

$$B_o = \frac{62.4\gamma_o + 0.0136 \cdot GOR \cdot \gamma_g}{\rho_o}, \quad (10)$$

where B_o is the formation volume factor, ρ_o is the density of the oil in lbm/ft^3, and γ_o and γ_g are the STO and gas specific gravities, respectively. The values of formation volume factor were computed at multiple temperatures and pressures from the measured values of live-oil density, GOR, and specific gravities. A mapping function was constructed to relate the calculated B_o to normalized T_1, T_2, and D distributions, T and P. The comparison of values of B_o predicted using the leave-one-out method and the values calculated exactly from Eq. 10 is shown in Fig. 12. The values of B_o are predicted to within an average accuracy of 3.7%.

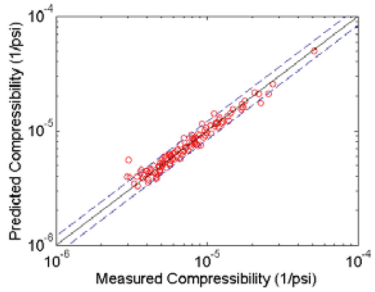

Fig. 11—Comparison of live-crude-oil compressibilities predicted from T_1, T_2, and D distributions, T, and P using the RBF mapping function method with the values measured in the laboratory. The solid black line is the equal-value line and the blue dashed lines are located at 20% deviation. The compressibilities are predicted to within 8.4% accuracy over the entire range.

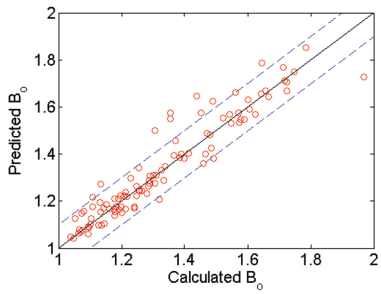

Fig. 12—Comparison of formation volume factor of live oils predicted from T_1, T_2 and D distributions, T, and P using the RBF mapping function method with the calculated values. The solid black line is the equal-value line and the blue dashed lines are located at 10% deviation. The formation volume factors are predicted to within an average accuracy of 3.7%.

GOR. GOR is an important fluid property for material selection of well completions, design of surface facilities, and optimization of production techniques. GOR is not a pressure- and temperature-dependent property. Hence, the measurements made on a live-crude oil at multiple temperatures and pressures map to a single GOR value in the output space. As a result, the effective size of the database is the number of live crude oils in the database.

GOR was predicted from the mapping function methodology using normalized T_1, T_2, D distributions, and normalized T and P as inputs. Figure 13 shows the comparison of the GOR predicted using the leave-one-out method with the measured values. The optimal α is 3.0 in this case. GOR is predicted to within an average accuracy of 17.2%. The accuracy of the predictions is expected to significantly improve for a larger database with, for example, 30 crude oils.

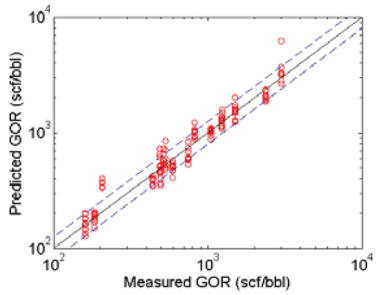

Fig. 13—Comparison of GOR of live-crude oils predicted from T_1, T_2, and D distributions, T, and P using the mapping function method with the values measured in the laboratory. Note that the spread along the y-axis for each x-value corresponds to the predicted GOR from measurements at different T and P. The solid black line is the equal-value line and the blue dashed lines are located at 20% deviation. The GORs are predicted to within an average accuracy of 17.2%.

Molecular Composition. The NMR relaxation time and diffusion distributions of live-crude oils contain information on molecular composition of crude oils. The smaller molecules in a crude-oil mixture have large diffusion coefficients and long relaxation times, and vice versa. However, the relationship between molecular composition and NMR distributions is a complex function of the multitude of inter- and intra-molecular interactions between the different types of molecules present in the crude oil. Such complex interactions cannot be accurately described by simple idealized models.

The molecular composition of live crude oils was predicted from the mapping function methodology using normalized T_1, T_2, D distributions and normalized T and P as inputs. Because molecular composition is not a temperature- and pressure-dependent property, the effective size of the database is the number of live-crude oils in the database. Figure 14 shows the comparison of methane, ethane, and

propane compositions predicted from the mapping function methodology with those measured using laboratory GC. For methane, the widths were kept fixed ($s_i = 4.0$) whereas for the other components, the widths were obtained from Eq. 8. The average absolute accuracies for the prediction of C_1, C_2, and C_3 are 1.0, 0.62, and 0.63 wt%, respectively. The components C_4-C_{29}, C_{30+} are predicted within an average absolute accuracy of 0.54 and 3 wt%, respectively. The scatter in the predictions arises because of the small effective size of the database.

Figure 15 shows the molecular compositions predicted from the mapping function for four live-crude oils in the database. The molecular compositions are obtained by averaging the predictions at multiple temperatures and pressures. The horizontal bars above and below the predicted value for each component correspond to the maximum and minimum predicted values. The vertical lines, therefore, represent the spread in the predictions at multiple temperatures and pressures. For comparison, the molecular composition measured by GC in the laboratory is also shown. Good quantitative agreement between predicted and measured composition is observed for all oils.

SARA Fractions. The SARA fractions are used to characterize crude oils in four classes of varying polarizability. Figure 16 shows the comparison of SARA fractions predicted using the mapping function method with SARA fractions measured in the laboratory for nine typical oils in the database.

The vertical bars in the Fig. 16 correspond to the range of values predicted for each component at different temperature and pressure conditions. The input vector, $\overrightarrow{A_T}$, included normalized amplitudes of T_1, T_2, and D distributions, normalized T and P. The widths were determined such that α in Eq. 8 was equal to 0.5. The SARA fractions are predicted within an average absolute accuracy of 7.0, 3.6, 6.4, and 0.48 wt%, respectively. It should be noted that live-oil NMR responses were used to predict the dead-oil SARA using an RBF mapping function. We found that the addition of the D distribution in the input vector did not improve the accuracy of the asphaltene predictions. This conclusion is consistent with the result that D distributions of oils are not affected by the presence of asphaltenes (Hurlimann et al., 2009).

Integration of NMR and NIR Optical-Density Measurements

The mapping function methodology allows a straightforward integration of different types of measurements for prediction of fluid properties. The integration is easily performed by including the optics and NMR measurements in the input vector. The integration does not add any additional complexity to the computations.

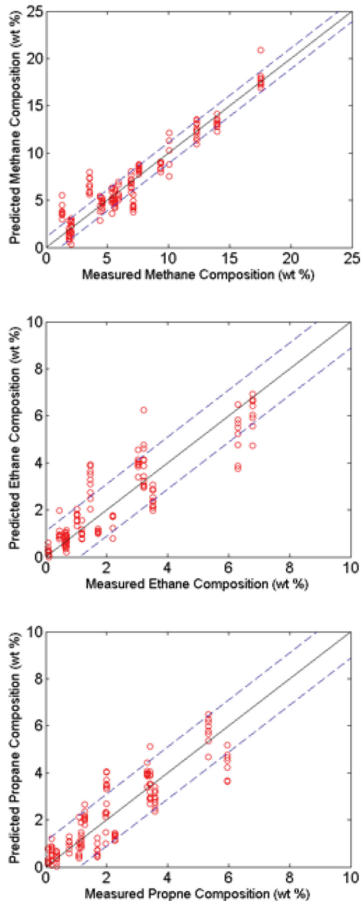

Fig. 14—Comparison of methane, ethane and propane compositions of live-crude oil predicted from T_1, T_2, and D distributions, T, and P using the mapping technique with the values measured in the laboratory. Note that the spread along the y-axis for each x-value corresponds to the predicted C_1, C_2, and C_3 from measurements at different T and P. The solid black line is the equal-value line and the blue dashed lines are located at 1 wt% deviation. Methane, ethane and propane compositions are predicted to within 1.0, 0.62, and 0.63 wt%, respectively.

The NIR optical-density (OD) spectra of the live oils in the database for wavelengths in the range from 1,500 to 2,000 nm were used in the integration. The optical absorption in this wavelength range is dominated by molecular vibrations in hydrocarbons. Fluid properties were predicted from the RBF mapping function in Eq. 2. The input vector consisted of normalized amplitudes of T_1, T_2, D distributions, OD, and normalized T and P:

$$\overrightarrow{A_T} = \overrightarrow{A_T}(A(T_1), A(T_2), A(D), OD, T, P). \quad (11)$$

As was noted previously, the shape of the absorption spectra of live oils is independent of temperature and pressure; however, the amplitudes of the spectra change with temperature and pressure. Therefore, for temperature- and pressure-independent properties such as molecular

composition and GOR, the absorption spectra were normalized with the largest amplitude in order to remove the temperature and pressure dependence. For temperature- and pressure-dependent properties such as compressibility, density, and viscosity, the spectra were not normalized to preserve the temperature and pressure dependence. No significant improvement in the predictions of oil viscosity, density, compressibility, formation volume factor, and GOR was observed by integration of NMR and optical-density measurements. A small improvement in the predictions of the C_1 weight fraction was observed with the integration of NMR distributions and OD spectrum. The weight fraction of C_1 was predicted to within an average accuracy of 0.88 wt%, compared with 1.0 wt% average accuracy with NMR distributions alone. However, no improvement was observed in the predictions of molecular fractions C_2 and higher by the integration of NMR and OD measurements. These results clearly show that NMR distributions contain much more information on molecular composition and other fluid properties than do the NIR OD measurements.

CONCLUSIONS

This paper has significantly raised the bar in several important areas related to NMR reservoir fluid characterization and NMR instrumentation. The topics discussed in the paper include the following: (1) an extensive database of NMR, optical density, and fluid-properties measurements acquired at multiple temperatures and pressures up to 175°C and 25,000 psi, (2) an innovative high-performance NMR laboratory system used to perform the high-pressure and high-temperature measurements, and (3) the prediction of fluid properties such as viscosity, density, compressibility, molecular composition, GOR, and SARA from NMR measurements and the accuracies of those predictions.

This paper shows, for the first time, that NMR measurements can be used to accurately determine molecular composition (C_1-C_{29}, C_{30+}), SARA fractions, GOR, viscosity, compressibility, density, and formation volume factor. We show that accurate fluid properties can be quantitatively predicted from a database of NMR and fluid-properties measurements using a model-independent mapping function method derived from radial-basis functions. Integrating the NMR and optics measurements resulted in essentially no improvement in the predicted compositions. The accuracies, of the fluid properties, predicted from the NMR measurements are shown in Table 1.

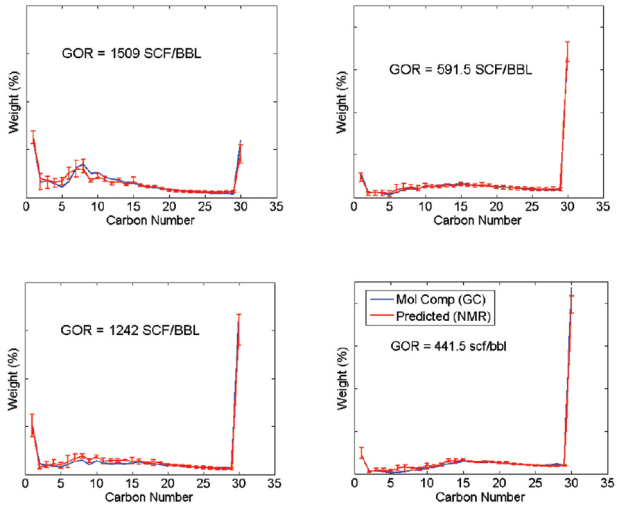

Fig. 15—Comparison of molecular compositions of four typical live-crude oils in the database predicted from T_1, T_2, and D distributions, T, and P using the RBF mapping method with the values measured in the laboratory using GC.

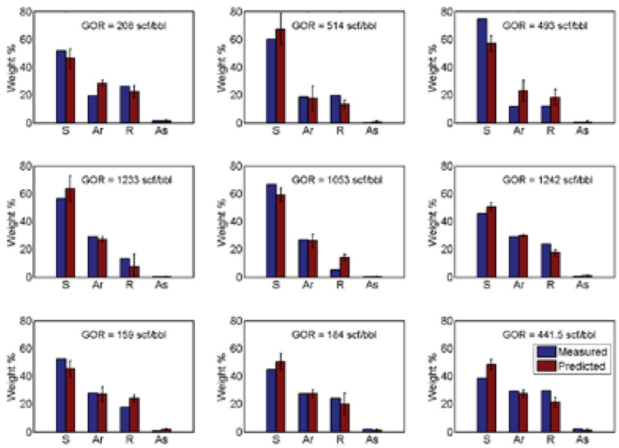

Fig. 16—Comparison of SARA fractions of nine typical live-crude oils in the database predicted from T_1, T_2, and D distributions, T, and P using the RBF mapping method with the values measured in the laboratory.

Table 1—Summary of NMR Fluid Properties Predictions

Fluid Property	Database Ranges of Fluid Properties	Accuracy of NMR Prediction
C_1 (wt%)	1.3–17.6	1
C_2 (wt%)	0.08–6.8	0.62
C_3 (wt%)	0.07–5.9	0.63
C_4-C_{29} (wt%)	1.6–3.2	0.54
C_{30+} (wt%) (wt%)	7.7–47.3	3
Saturates (wt%)	38.7–74.6	7.0
Aromatics (wt%)	11.7–30.5	3.6
Resins (wt%)	5.3–29.4	6.4
Asphaltenes (wt%)	0.1–2.2	0.48
GOR (scf/bbl)	150–3,000	17.2%
Viscosity (cp)	0.1–80	10.6%
Compressibility (10^{-6} psi^{-1})	3–40	8.4%
Density (g/cm^3)	0.43–0.93	0.019
Formation volume factor	1.05–1.95	3.7%

ACKNOWLEDGMENTS

It is a pleasure to acknowledge productive discussions with our colleagues Richard Harris, Bruno Jorion, Nate Bachman, and Nick Heaton during the course of this work. Bruno Luong helped with the magnet modeling. Thanks to Dexter Magnetics for their help with the design, modeling, and building of the magnet. We also thank Schlumberger for permission to publish this work.

NOMENCLATURE

$\vec{A}$ = normalized amplitudes of a T_1, T_2, or D distribution, dimensionless
$\vec{A}_j$ = normalized amplitudes of a T_1, T_2, or D for j-th database measurement, dimensionless
$\vec{A}_T$ = vector containing the normalized input measurements, dimensionless
$\vec{A}_{T,i}$ = vector containing the normalized input measurements for the i-th database measurement, dimensionless
a_s = radius of a diffusing particle, cm
B_o = oil formation volume factor, dimensionless
$\vec{c}_i$ = coefficient vector multiplying RBF function, units of $\vec{F}(\vec{x})$
D = molecular diffusion coefficient, $cm^2 \cdot s^{-1}$
$\vec{F}(\vec{x})$ = RBF mapping function, units of predicted fluid property
g = applied pulsed field gradient amplitude, G/cm
GOR = gas/oil ratio, scf/bbl
I_o = intensity of incident infrared radiation
I_t = intensity of transmitted infrared radiation
k_B = Boltzmann's constant, $cm^2 \cdot g \cdot s^{-2} \cdot K^{-1}$
N = number of measurements in database
N_c = number of components in input measurement vector
NN_i = nearest neighbor distance for database inputs, dimensionless
OD = near-infrared optical density, dimensionless
P = pressure, psi
s_i = width of Gaussian RBF centered at database input $\vec{x}_i$, units of $\vec{x}_i$
T = temperature, degrees Kelvin
T_1 = longitudinal relaxation time, sec
T_2 = transverse relaxation time, sec
$< T_1 >$ = logarithmic mean value of T_1 distribution, sec
$< T_2 >$ = logarithmic mean value of T_2 distribution, sec
$\vec{x}$ = N_c-dimensional input vector
$\vec{x}_i$ = N_c-dimensional input vectors in database for $i = 1,2,..., N$
$x_{k,i}$ = k-th component of the i-th database measurement, $\vec{x}_i$
x_k = k-th component of input vector $\vec{x}$
α = proportionality constant that multiplies nearest neighbor distances, dimensionless
β = isothermal compressibility, psi^{-1}
δ = width of pulsed field gradient pulses, sec
Δ = diffusion time in pulsed field gradient measurements, sec
η = viscosity, cp
λ = coefficient relating D and T_2 for dead oils, $cm^2 \cdot s^{-2}$
γ_g = gas specific gravity, dimensionless
γ_o = oil specific gravity, dimensionless
ρ_o = oil density, lbm/ft^3

REFERENCES

Akkurt, R., Vinegar, H., Tutunjian, P.N., and Guilloy, A.J., 1996, NMR Logging of Natural Gas Reservoirs, *The Log Analyst*, **37**(6), 33-42.

Anand V., and Freedman, R., 2012, New Method for Predicting Properties of Live Oils From NMR, *Petrophysics*, **53**(4), 256-271.

Coates, G., Xiao, L., and Prammer, M., 1999, *NMR Logging: Principles and Applications*, Gulf Publishing Company, Houston, Texas.

Freedman, R., 2006a, New Approach for Solving Inverse Problems Encountered in Well-Logging and Geophysical Applications, *Petrophysics*, **47**(2), 93-111.

Freedman, R., 2006b, Method and Apparatus for Using Pulsed Field Gradient Measurements to Determine Fluid Properties in a Fluid Sampling Tool, US Patent No. 7,053,611.

Freedman, R., Anand, V., Zhou, T., Rose, D., and Beekman, S., 2012, A Modern Method for Using Databases to Obtain Accurate Solutions to Complex Reservoir Characterization Problems, Paper SPE-147169, *SPE Reservoir Evaluation and Engineering*, **15**(4), 453-461.

Freedman, R., Cao Minh, C., Gubelin, G., Freeman, J.J., McGinness, T., Terry, B., and Rawlence, D., 1998, Combining NMR and Density Logs for Petrophysical Analysis in Gas-Bearing Formations, Paper II, *Transactions, SPWLA 39th Annual Logging Symposium*, Keystone, Colorado, USA, 26-29, May.

Freedman, R., and Ganesan, K., 2007, Method for Determining More Accurate Diffusion Coefficient Distributions of Reservoir Fluids Using Bipolar Pulsed Field Gradients, US Patent No. 7,253,618.

Freedman, R., Lo, S., Flaum, M., Hirasaki, G.J., Matteson, A., and Sezginer, A., 2001, A New Method of Fluid Characterization in Reservoir Rocks: Experimental Confirmation and Simulation Results, Paper SPE-75325, *SPE Journal*, **6**(4),452-464.

Freedman, R., and Heaton, N., 2004, Fluid Characterization Using Nuclear Magnetic Resonance Logging, *Petrophysics*, **45**(3), 241-250.

Prammer, M. G., Bouton, J., and Masak, P., 2001, The Downhole NMR Fluid Analyzer, Paper N, *Transactions*, *SPWLA 42nd Logging Symposium*, Houston, Texas, USA, 17-20 June.

Harris, K.R., 1982, Temperature and Density Dependence of the Self-Diffusion Coefficient of *n*-Hexane From 223 to 333 K and Up to 400 MPa, *Journal of the Chemical Society Faraday Transactions I*, *Physical Chemistry in Condensed Phases*, **78**, 2,265-2,274.

Hurlimann, M.D., Freed, D.E., Zielinski, L.J., Song, Y.Q., Leu, C., Straley, C., Cao Minh, C., and Boyd, A., 2009, Hydrocarbon Composition From NMR Diffusion and Relaxation Data, *Petrophysics*, **50**(2), 116-129.

Krynicki, K., Green, D.C., and Sawyer, D.W., 1978, Pressure and Temperature Dependence of Self-diffusion in Water, *Faraday Discussions of the Chemical Society*, **66**, 199-208.

Lo, S.-W., Hirasaki, G.J., House, W.V., and Kobayashi R., 2000, Correlations of NMR Relaxation Time With Viscosity, Diffusivity, and Gas/oil Ratio of Methane/ Hydrocarbon Mixtures, Paper SPE-63217, presented at the SPE Annual Technical Conference and Exhibition, Dallas, Texas, USA, 1-4 October.

Looyestijn, W. J., 1996, Determination of Oil Saturation from Diffusion NMR Logs, Paper SS, *Transactions*, *SPWLA 37th Annual Logging Symposium*, New Orleans, USA, 16-19, June.

Stejskal E.O. and Tanner J.E. 1965, Spin Diffusion Measurements: Spin Echoes in the Presence of a Time-Dependent Field Gradient, *Journal of Chemical Phys*ics, **42**(1), 288–92.

Vold, R.L., Vold, R.R., and Simon, H.E., 1969, Errors in Measurements of Transverse Relaxation Times, *Journal of Magnetic Resonance*, **11**, 283-298.

Von Meerwall, E., Beckman, S., Jang, J., and Mattice, W.L., 1998, Diffusion of Liquid *n*-Alkanes, Free-Volume and Density Effects, **108**(10), *Journal of Chemical Physics*, 4,299-4,304.

Winkler, M., Freeman, J. J. and Appel, M., 2004, The Limits of Fluid Property Correlations Used in NMR Well Logging: An Experimental Study of Reservoir Fluids at Reservoir Conditions, Paper DD, *Transactions*, *SPWLA 45thAnnual Logging Symposium*, Noordwijk, The Netherlands, 6-9 June.

Zhang, Y., Hirasaki, G. J., House, W. V., and Kobayashi, R., 2002, Oil and Gas NMR Properties: The Light and Heavy Ends, Paper HHH, *Transactions*, *SPWLA 43rdAnnual Logging Symposium*, Oiso, Japan, 2-5, June.

Zielinski, L. and Hurlimann, M.D., 2011, Nuclear Magnetic Resonance Dispersion of Distributions as a Probe of Aggregation in Crude Oils, *Energy & Fuels*, **25**, 5,090-5,099.

ABOUT THE AUTHORS

Bob Freedman is a Scientific Advisor in Schlumberger's Houston Formation Evaluation Center in Sugar Land, TX. Bob holds a PhD in physics from the U. of California at San Diego, and was awarded Post-Doctoral Fellowships in physics at the Xerox Palo Alto Research Center and at the University of Chicago. He has worked for Schlumberger for 28 years. Prior to joining Schlumberger Bob worked for five years in operations and research for Shell and for five years as an independent formation evaluation consultant. During his 38-year oil industry career he has published 60 SPE, SEG, and SPWLA papers in many different areas of formation evaluation and has been granted more than 35 U.S. patents on well logging technology. Bob played a leading role in the development of Schlumberger's Pulsed NMR Logging Tool technology. He has won many top paper awards for papers presented at SPE, SPWLA, and at internal Schlumberger technical conferences. Bob's work has been recognized by both the SPE and SPWLA and he served as a Distinguished Lecturer for both organizations and also as a Distinguished SPE Author. He served as the Vice-President of Technology for the SPWLA in 2008. He received a 2009 SPWLA Award for Distinguished Technical Achievement and also was awarded a 2004 SPE Cedric Ferguson Certificate.

Vivek Anand is a Senior Research Scientist and Manager of Interpretation Engineering for NMR Answer Products at Schlumberger Sugar Land product center. Vivek obtained a BS degree from Indian Institute of Technology, New Delhi in 2002 and a PhD from Rice University, Houston in 2007, both in Chemical Engineering. At Schlumberger, his research interests include NMR in porous media, fluid characterization, and mathematical modeling. He was a SPWLA Distinguished Speaker for 2009, the recipient of best paper award for the 2005 SPWLA Annual Symposium, and the 2011 SPE Young Professional Best Paper Award.

Daniel Catina has been an Embedded Software Engineer for eight years specializing in the development of new oil exploration tools. He worked at Schlumberger for five years and is currently employed

at National Oilwell Varco. He enjoys debugging firmware and hardware and coding in C, but also works in Assembly, C++, Java, MatLab and Python. He received his bachelor's degree in Computer Systems engineering from the University of Houston. Daniel can be reached at dcatina@hotmail.com.

Bill Grant is a consulting mechanical engineer (MS from Texas A&M University) with 25 years of experience in the design of well-logging tools and other oilfield hardware and is a registered professional engineer (PE) in the state of Texas. Bill has a broad range of expertise including fluid-sampling tool design, hydraulics, microfluidics, hydraulic-system modeling, and overall system design. His experience also includes firmware development, control-systems design, and corrosion-resistant materials. Bill has been granted nine U.S. patents on his hardware designs. He currently manages his own design and consulting firm and can be contacted at bill@grantinnovation.com.

Payam Tabrizi, P.E., is currently a Senior Electrical Engineer with Schlumberger designing downhole electronics. In 2006, he joined Schlumberger Oilfield Services as a field engineer where he provided various openhole wireline services for the Mexican national oil company, PEMEX. In 2008, he began his career as a design engineer at the Schlumberger Product Center in Houston where he has worked on induction and NMR downhole tools for both wireline and LWD. His areas of expertise include low-noise analog design, digital acquisition and processing, and high-temperature electronic design and packaging for downhole logging tools. He received his BS and MS degrees in electrical engineering from the University of Texas at Austin in 2004 and 2006, respectively. In 2012, he became a licensed Professional Engineer in the state of Texas.

Ricky Torres is a Senior Development Electronic Technician who has worked in Schlumberger Engineering for 37 years. He holds a BS degree in Electronics Engineering Technology from the DeVry Institute of Technology in Dallas, Texas. Ricky has considerable experience and expertise in the development of analog circuitry from the audio-frequency range to the low gigahertz-frequency range. His expertise includes the troubleshooting of digital systems using microprocessors, digital signal processors, field programmable gate arrays, and other complex digital hardware. Ricky is recognized within Schlumberger as one of the foremost company experts in solving grounding, shielding, and crosstalk problems in complex electronic systems.

Krishnamurthy Ganesan is an NMR experimental physicist with Schlumberger who has worked in the field of NMR for the last 35 years. He has a PhD degree in NMR physics from Indian Institute of Science, Bangalore, India. He joined Schlumberger in 1996 to work on the LWD NMR proVISION tool. He has developed a novel azimuthal NMR imaging technique for the logging tool. He has 25 U.S patents relating to NMR logging tool sensors and techniques. He worked as a research faculty at the physics department, University of Utah for 11 years before joining Schlumberger. He taught graduate-level instrumentation courses and worked on lung MRI at the University of Utah.

Craig Borman, a Chemical Engineering Technologist at the Schlumberger DBR Technology Center, Edmonton, Canada, has over 19 years experience in fluids analysis, experimental design and sensor qualification. He spent many years designing laboratory equipment and experimental procedures in the area of thermodynamics, fluid property characterization and solids analysis. As a Principal technical expert in his domain he has made many "impossible" experiments a success by carefully designing the experiments and modifying the high pressure PVT equipment in unique ways to obtain excellent results. Craig has been a key contributor in the development of fluids related training programs and has mentored many other fluid analysis experts.

C. (Brad) Krueckl has worked in reservoir fluid analysis for the last 13 years. He spent three years with Core labs before taking a position with Schlumberger in Houston. Brad spent nine years in Houston in various capacities, ranging from lab tech, special projects team, shift leader, and finally for the last three years there he was EIC/lab supervisor. Brad was also involved in RSA global standardization of procedures. In 2012 he transferred to Edmonton to work in the engineering

group (NPD) at the Schlumberger DBR Technology Center.

Darcy Ryan is the Engineering and Sustaining Manager at the Schlumberger DBR Technology Center in Edmonton, Canada. He is a registered professional engineer in Canada. Darcy obtained a BS degree in 1997 and a Masters of Engineering degree in 1999 from the University of Alberta, both in Electrical Engineering with a focus on embedded systems development. Following graduation he worked as an engineer before joining Schlumberger in 2002. During his career at Schlumberger Darcy has been worked on artificial lift, submersible pump power and control systems, reservoir monitoring and control gauges, laboratory fluid analysis, and downhole tool-measurement validation.